05,07

Effect of the concentration of the substitution impurity strontium on the magnetic ordering temperature in $La_{1-x}Sr_xFeO_{3-\delta}$ and its sensitivity to heat treatment

© A.I. Dmitriev[1], S.V. Zaitsev[2], M.S. Dmitrieva[1]

[1] Federal Research Center of Problems of Chemical Physics and Medicinal Chemistry RAS, Chernogolovka, Russia
[2] Osipyan Institute of Solid State Physics RAS, Chernogolovka, Russia

E-mail: aid@icp.ac.ru

Received October 27, 2024
Revised December 17, 2024
Accepted December 17, 2024

The dependences of magnetization on temperature of $La_{1-x}Sr_xFeO_{3-\delta}$ ($x = 0.33$, 0.50, 0.67) samples before and after vacuum heat treatment are studied. The Néel temperature T_N, at which weak noncollinear ferromagnetism is established, is determined for each sample. The introduction of a substitutional Sr impurity into $La_{1-x}Sr_xFeO_{3-\delta}$ leads to a decrease in T_N. This effect is compensated by vacuum heat treatment, during which an increase in TN is observed. Antiferromagnetic ordering at room temperature in annealed samples is confirmed by the presence of an intense Raman peak of two-magnon scattering at 1360 cm^{-1} in the Raman spectra.

Keywords: Substituted lanthanum orthoferrites, canted antiferromagnetism, vacuum annealing.

DOI: 10.61011/PSS.2025.01.60594.282

1. Introduction

Substituted orthoferrites $La_{1-x}Sr_xFeO_{3-\delta}$ ($0 \le x \le 1$) exhibit interesting changes in their physical properties depending on the composition [1]. Lanthanum orthoferrite $LaFeO_3$ is at one edge of this series of compounds at $x = 0$. It is an antiferromagnetic insulator with the highest Néel temperature of $T_N = 740$ K in the orthoferrite family [1]. $LaFeO_3$ is a promising functional material due to its excellent optical, electrical, magnetic, and chemical properties [2]. In particular, it is one of the few single-phase multiferroid materials with both antiferromagnetic and ferroelectric properties. $LaFeO_3$ has great potential for applications in computer chips, smart sensors, electronic spin devices, and catalysis [2]. Strontium orthoferrite $SrFeO_3$ is on the other side of this family at $x = 1$. It is an antiferromagnetic metal with a Néel temperature of $T_N = 134$ K [1]. In the latter case, a reversible phase transition from the perovskite structure of $SrFeO_3$ to the brownmillerite structure of $SrFeO_{2.5}$ is observed, accompanied by a switching of electrical resistance and forming the basis for the creation of high-performance artificial synapses for neuromorphic computing [3]. There is a whole family of substituted orthoferrites $La_{1-x}Sr_xFeO_{3-\delta}$ with a rich variety of structures and promising properties between the „pure" orthoferrites of lanthanum and strontium. In particular, $La_{1-x}Sr_xFeO_{3-\delta}$ is promising for practical use as a material absorbing electromagnetic waves, the operating frequency of which can be finely tuned depending on x [4]. Replacing the trivalent ion La^{3+} with the divalent ion of strontium Sr^{2+} can significantly change the magnetic and electron transport properties of $La_{1-x}Sr_xFeO_{3-\delta}$, demonstrating various effects of magnetic and charge orderings [4]. The purpose and novelty of this study is to establish the dependence of the temperature of the magnetic ordering in $La_{1-x}Sr_xFeO_{3-\delta}$ on the concentration of a substitutive impurity of strontium $T_N(x)$ and to identify possible mechanisms determining its occurrence.

2. Methodology and samples

Polycrystalline samples $La_{1-x}Sr_xFeO_{3-\delta}$ ($x = 0.33$, 0.50, 0.67) were synthesized by the sol-gel method using Sr, Fe, and La nitrates in a stoichiometric ratio as initial reagents. They will be further designated as Sr33, Sr50 and Sr67. The details of sample preparation, their composition and structure are described in Refs. [5–7]. Sr33 sample has an orthorhombic structure with lattice parameters $a = 5.502$ Å, $b = 5.544$ Å, $c = 7.811$ Å [5]. Sr50 sample has a rhombohedral structure with lattice parameters $a = 5.511$ Å, $c = 13.437$ Å in hexagonal axes ($a = 5.494$ Å and $\alpha = 60.20°$ in rhombohedral axes) [6]. Sr67 sample also has a rhombohedral structure with lattice parameters $a = 5.483$ Å, $c = 13.408$ Å in hexagonal axes ($a = 5.475$ Å and $\alpha = 60.07°$ in rhombohedral axes) [7].

The dependences of magnetization on temperature $M(T)$ were measured using CFMS vibration magnetometer (Cryogenic Ltd, UK) in a magnetic field with a strength of 1 kOe in the heating mode. The samples were cooled in a magnetic field with a strength of 10 kOe before the measurements.

Raman scattering (RS) spectra were recorded at room temperature in backscattering geometry. A laser with a wavelength of 532 nm and a laser radiation power of ~ 3 mW was used for excitation. The diameter of the laser spot on the sample focused by a microscopic lens ($\times 20$) was 5 μm. The laser line was suppressed by using a step filter of anti-Stokes' cut-off placed upstream of the spectrometer. The spectral accuracy and resolution in the studied frequency range were $\sim 1\,\mathrm{cm}^{-1}$.

3. Results and their discussion

Figure 1 shows the temperature dependences of the magnetization $M(T)$ of samples of Sr33, Sr50, and Sr67 before heat treatment. Curves similar to those shown in Figure 1 were previously observed in substituted orthoferrites $La_{1-x}Sr_xFeO_{3-\delta}$ with the antiferromagnetic structure [8]. Spins therein are arranged antiparallel due to a antiferromagnetic bond between two neighboring ferrum ions via an intermediate ion of oxygen. However, the samples exhibit non-collinear antiferromagnetism (weak ferromagnetism) due to the slight deviation of the spins from the strict antiparallel orientation resulting from the zigzag arrangement of oxygen octahedra containing iron ions.

$M(T)$ curves of Sr50 and Sr67 samples clearly exhibit Néel temperatures $T_N = 230$ K and 196 K, respectively (Figure 1). The values of T_N in the Sr50 and Sr67 samples were determined based on the extremum of the temperature dependence of the derivative dM/dT. The Néel temperature T_N is not clearly visible on the curve $M(T)$ of the Sr33 sample, since it exceeds the temperature range available to us, limited by the value $T = 380$ K. Therefore, it was determined by the method of approximating the curve $M(T)$ in the region of transition to a magnetically ordered state by the expression $M(T) \sim (T_N - T)^{\beta}$. The Néel temperature

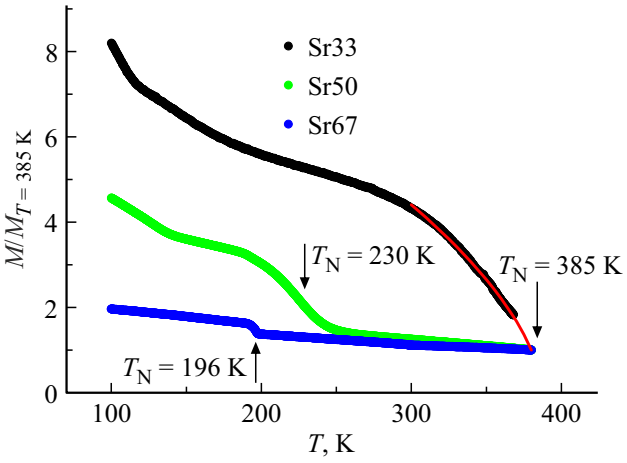

Figure 1. Normalized temperature dependences of magnetization $M/M_{T=380\,K}$ of samples Sr33 (black symbols), Sr50 (green symbols) and Sr67 (blue symbols). The arrows indicate Néel temperatures. The red line shows an approximation of the transition region to the magnetically ordered state of Sr33 sample.

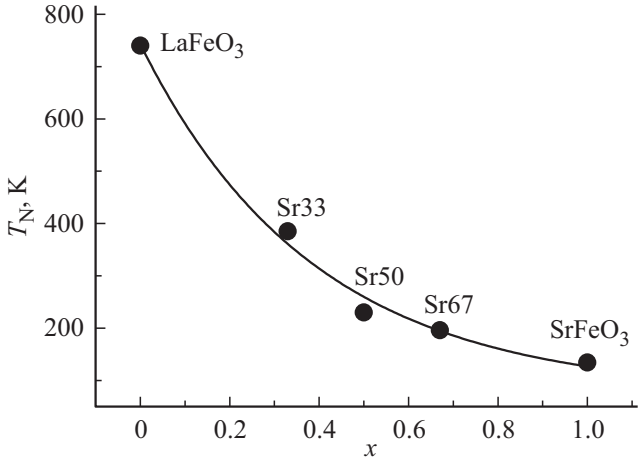

Figure 2. Dependence of the Néel temperature T_N in samples of $La_{1-x}Sr_xFeO_{3-\delta}$ on the concentration of the strontium substitutive impurity x. Solid line — spline.

T_N was 385 K for Sr33 sample. Thus, it can be seen that the temperature of the magnetic ordering of the compound $La_{1-x}Sr_xFeO_{3-\delta}$ decreases with the increase of x (Figure 2).

Let us now discuss the possible causes and mechanisms of the effect of a substitutive impurity of strontium on the magnetic properties of $La_{1-x}Sr_xFeO_{3-\delta}$. The temperature of the magnetic ordering is determined by the superexchange interaction between iron ions $V_{ex} = \Sigma J_{mn}(\mathbf{S_m} \cdot \mathbf{S_n})$ and is described by the simple relation $T_N = zS(S+1)J_{mn}/3k_B$ within the framework of the mean field approximation. A number of factors may be responsible for the change of the exchange integral J_{mn} and, accordingly, the temperature of the magnetic ordering. Oxygen vacancies are formed in $La_{1-x}Sr_xFeO_{3-\delta}$ in case of substitution, the number δ of these oxygen vacancies linearly increases with the increase of x [5–7]. The energy of the exchange interaction is proportional to the number of nearest neighbor pairs z (exchange bonds). An oxygen vacancy in the immediate environment of Fe^{3+} ion leads to a break of the exchange bond, which means a weakening of the superexchange interaction between iron ions and, consequently, a decrease of the Néel temperature, which is observed in experiments. However, the following contradiction draws attention to itself. Vacuum heat treatment of the samples leads to an additional increase of the number of oxygen vacancies δ, which means an increase of the number of broken exchange bonds. This should lead to a decrease of the Néel temperature as a result of heat treatment, while the exact opposite situation is observed in experiments [9,10]. This suggests that the superexchange interaction between iron ions is more controlled by other factors.

The exchange integral depends on the degree of overlap of the wave functions, therefore it decreases exponentially with the increase of the distance between ions according to the expression $J_{mn} \sim \exp(-\alpha|r_m - r_n|)$, i.e. with the increase of the lengths of Fe–O, Fe–Fe bonds. A general

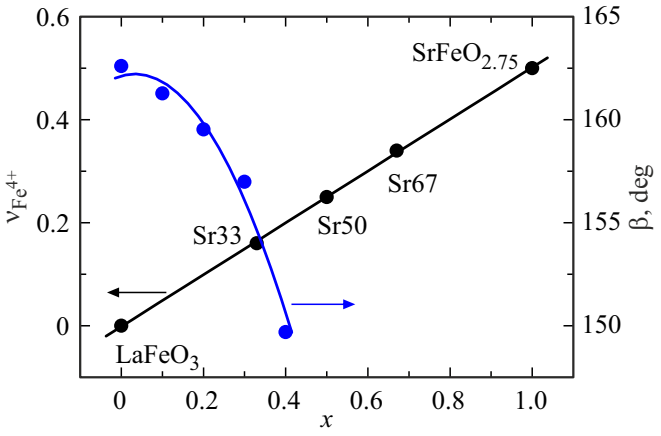

Figure 3. Dependences of the fraction of Fe^{4+} νFe^{4+} ions (black symbols) and the angle of Fe−O−Fe β bond (blue symbols) [4] on the concentration of the substitutive impurity of strontium x [5−7].

tendency of decrease of the volume of the perovskite cell V/z is observed for $La_{1-x}Sr_xFeO_{3-\delta}$ in case of substitution, which should be accompanied by a reduction of the length of Fe−O d bond with an increase of the amount of strontium x [1,5–7]. This should lead to an increase of the superexchange interaction between iron ions and, consequently, an increase of the Néel temperature in case of substitution with an increase of x. However, the opposite situation is observed in experiments. Variations in the lengths of Fe−O, Fe−Fe bonds also fail to explain experiments on vacuum heat treatment. The latter leads to an increase of the volume of the perovskite cell V/z, which should be accompanied by a corresponding increase of the length of Fe−O d bond [5–7,11]. The crystal lattice undergoes two mutually-dependent processes during vacuum annealing: the oxygen ion is removed with a vacancy formed, and the vacancy state of the ferrum ions changes from 4+ to 3+. The ions Fe^{4+} on Fe^{3+} have a different ionic radius, therefore, vacuum annealing changes the parameters of the crystal lattice. In this case, a weakening of the superexchange interaction between iron ions should be expected and, consequently, a decrease of the Néel temperature. Again, the exact opposite situation is observed in experiments. This indicates that the superexchange interaction between iron ions is more controlled by other factors. Among these, it remains to discuss the change of the angle Fe−O−Fe bond and the valence state of iron ions (Figure 3). It is known that changes of the crystal structure of $La_{1-x}Sr_xFeO_{3-\delta}$ when La^{3+} is replaced by Sr^{2+}, among other things, lead to a decrease of the angle of Fe−O−Fe β bond with the increase of x (Figure 3) [4].

The superexchange interaction increases with the increase of the angle of angle of Fe−O−Fe β bond according to the expression, $J_{mn} = A + B\cos\beta + C\cos^2\beta$, the microscopic derivation of which was obtained back in 1970 for ions with the configuration $3d^5$. The superexchange integral J_{mn} reaches a maximum at $\beta = 180°$ as can be seen from the last expression [4]. The parameters A, B and C depend on the cation-ligand separation here. A comprehensive analysis confirmed the correctness of the last expression for the dependency $J_{mn}(\beta)$. The second term in it is determined by interconfigurational $2p$-ns excitations of the ligand, while the other terms are associated with intraconfigurational contributions $2p$ and $2s$. It was later shown that the orbitally isotropic contribution to the superexchange integral for a pair of Fe ions^{3+} with configurations $t_{2g}^3 e_g^2$ can be written as follows for $3d$ ions in a strong crystal field of cubic crystals: $J_{mn} = (1/25)\big(4J(e_g e_g) + 12J(e_g t_{2g}) + 9J(t_{2g} t_{2g})\big)$. Here J are parameters related to electron transfer to partially occupied electron shells: $J(e_g e_g) = (t_{ss} + t_{\sigma\sigma}\cos\beta)^2/2U$, $J(e_g t_{2g}) = t_{\sigma\pi}^2 \sin^2\beta/3U$, $J(t_{2g} t_{2g}) = 2t_{\pi\pi}^2(2 - \sin^2\beta)/9U$, where $t_{ss}, t_{\sigma\sigma}, t_{\sigma\pi}$ are integrals of d−d transfer, U is the average value of energy of d−d transfer (correlation energy). Thus, the ion substitution in $La_{1-x}Sr_xFeO_{3-\delta}$ and growth x, reducing the angle of Fe−O−Fe 3) bond, weakens the antiferromagnetic superexchange interaction and thereby lowers the Néel temperature in exact agreement with the experiment. Variations of the angle of Fe−O−Fe bond can also explain the significant increase of Néel temperature as a result of heat treatment, which leads to a noticeable increase of β from 166° to = 174° (Figure 3) [11].

Let us now discuss the effect of variations of the valence state of iron ions in case of ion substitution and vacuum heat treatment of $La_{1-x}Sr_xFeO_{3-\delta}$ (Figure 3) [5–7]. The fractions of Fe^{3+} and Fe^{4+} ions were determined by Mossbauer spectroscopy [5–7]. The exchange interaction between Fe^{3+} and Fe^{3+} ions is antiferromagnetic according to Goodenough's superexchange theory, and it is stronger than the exchange interaction between Fe^{3+} and Fe^{4+} or Fe^{4+} and Fe^{4+} ions. Therefore, the introduction of Sr^{2+} ions into lanthanum orthoferrite, which generates Fe^{4+} ions, weakens the exchange interaction and, accordingly, lowers the temperature of the magnetic ordering. Subsequent vacuum heat treatment leads to the removal of oxygen ions with the formation of a vacancy which changes the valence state of iron ions from 4+ to 3+. On the contrary, t his enhances the exchange interaction and, accordingly, increases the temperature of the magnetic ordering.

Figure 4 shows the RAMAN spectra at room temperature of Sg33a, Sg50a, and Sg67a samples after heat treatment (10^{-3} Torr) at 650°C for 6 h. Sr33, Sr50, and Sr67 samples do not have magnon and phonon Raman peaks before heat treatment. The Raman spectra of unsubstituted lanthanum orthoferrite $LaFeO_3$ and the brownmillerite phase of strontium orthoferrite $SrFeO_{2.5}$ are also shown for comparison. The antiferromagnetic type of ordering at room temperature in the samples after heat treatment is indicated by the presence of a pronounced Raman peak of two-magnon scattering at 1300−1400 cm^{-1} in the Raman spectra (Figure 4) [12]. A strong two-magnon scattering line is observed in the spectrum of unsubstituted lanthanum ferrite $LaFeO_3$, which has the highest Néel temperature

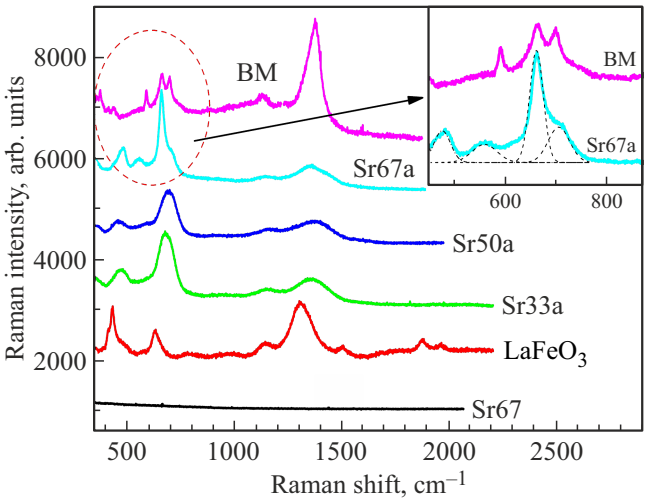

Figure 4. Raman spectra of Sg33a, Sg50a, and Sg67a samples after heat treatment, Sr67 sample before heat treatment, as well as unsubstituted lanthanum orthoferrite $LaFeO_3$ and the brownmillerite phase of strontium orthoferrite $SrFeO_{2.5}$. The spectra are sequentially shifted vertically. The inset shows the spectra of $SrFeO_{2.5}$ and Sr67a samples in the region of the strongest phonon mode at $660-700\,cm^{-1}$. Dashed lines — Gaussian fitting for Sr67a.

$T_N = 740\,K$ [1], as well as in the brownmillerite phase of strontium ferrite $SrFeO_{2.5}$ with $T_N = 670\,K$ [13].

Moreover, an intense two-phonon scattering line is present in the RAMAN spectra at $1150\,cm^{-1}$, which is manifested due to the strong coupling of the phonon and spin systems in these compounds [14]. Raman lines in the RS spectra of orthoferrites $La_{1-x}Sr_xFeO_{3-\delta}$ are caused by phonon oscillations at frequencies below $1000\,cm^{-1}$ [15]. For instance, the strongest phonon mode at a frequency of $660\,cm^{-1}$ describes in-phase oscillations of Fe−O bonds in the FeO_6 octahedron — the so-called „breathing" octahedron mode [15]. The significant broadening of all RSS lines in samples $La_{1-x}Sr_xFeO_{3-\delta}$ compared with unsubstituted lanthanum orthoferrite $LaFeO_3$ is naturally associated with a local disorder that occurs when lanthanum is substituted by strontium.

Figure 4 also shows the RS spectrum of the Sr67 sample before heat treatment, in which there are no magnon and phonon Raman peaks. The absence of a two-magnon scattering line in this sample indicates the absence of antiferromagnetic ordering at room temperature, which confirms the data of magnetometric studies (Figure 1). At the same time, the suppression of phonon modes related to vibrations in FeO_6 octahedron indicates a significant proportion of Fe^{4+} ions in the samples before heat treatment.

Attention is drawn to the more complex structure of the phonon mode of the octahedron FeO_6 at $660\,cm^{-1}$ in Sg67a sample after heat treatment. For convenience, it is shown on an enlarged scale in the box to Figure 4 along with a double line of this mode of approximately the same intensity in a sample of the brownmillerite phase $SrFeO_{2.5}$ (at $662\,cm^{-1}$ and $697\,cm^{-1}$). Fitting the spectrum of Sg67a sample with two Gaussians gives very close values of the frequencies of the components: $660\,cm^{-1}$ and $704\,cm^{-1}$ with an intensity ratio of 2:1 (their ratio is 2.15 after fitting), unlike the sample $SrFeO_{2.5}$. Such a close correspondence of the frequencies of the components of this phonon mode and the different ratio of their intensities in these two samples is not accidental. The fact is that iron ions are in the trivalent state of Fe^{3+}, and have two local oxygen environments in the $SrFeO_{2.5}$ sample, like in the substituted strontium orthoferrite $La_{0.33}Sr_{0.67}FeO_{3-\delta}$ after heat treatment (sample Sr67a): octahedral $Fe^{3+}(O)$ and tetrahedral $Fe^{3+}(T)$. This was shown by detailed studies of the structural features and valence states of iron using X-ray diffraction and Mossbauer spectroscopy for various conditions of synthesis and heat treatment of samples in the works [5–7]. The partial fraction of Mossbauer spectra corresponding to each of the environments, $Fe^{3+}(O)$ and $Fe^{3+}(T)$, is 44% and 50%, respectively, in the $SrFeO_{2.5}$ sample (the remaining 6% correspond to impurities of the rhombic phase $SrFeO_{2.75}$) [6]. The ratio of octahedral and tetrahedral environments in the Mossbauer spectra is 65% and 31%, respectively, in the Sr67a sample after heat treatment (4% correspond to the rhombic phase) [7]. Thus, the data of the Mossbauer and Raman spectroscopy on the ratio of the partial components of the spectra are in almost perfect agreement with each other. It is assumed that the octahedral environment of $Fe^{3+}(O)$ corresponds to the phonon mode of in-phase oscillations of Fe−O bond of the octahedron FeO_6 with a Raman frequency of $660-662\,cm^{-1}$, and the tetrahedral environment of $Fe^{3+}(T)$ has a higher oscillation frequency $\sim 700\,cm^{-1}$.

4. Conclusion

Thus, it was found in this study that a magnetic-ordered state of the type of a skewed antiferromagnet is formed at temperatures below the Néel temperature T_N in samples of $La_{1-x}Sr_xFeO_{3-\delta}$ ($x = 0.33, 0.50, 0.67$). The introduction of a substitutive impurity of strontium into $La_{1-x}Sr_xFeO_{3-\delta}$ and an increase of its concentration leads to a significant decrease of temperature T_N. The observed variations of the latter are explained by changes of the valence state of iron ions and the angles of Fe−O−Fe bond in case of substitution. The antiferromagnetic type of ordering is also indicated by the presence of a pronounced Raman peak of two-magnon scattering in the RS spectra at $1300-1400\,cm^{-1}$.

Acknowledgments

The authors would like to thank V.D. Sedykh and O.G. Rybchenko for providing samples and stimulating discussions.

Funding

This study was conducted under State Assignments of the Federal Research Center for Problems of Chemical Physics and Medical Chemistry (124013100858-3) and the Osipyan Institute of Solid State Physics.

Conflict of interest

The authors declare that they have no conflict of interest.

References

[1] J. Blasco, B. Aznar, J. García, G. Subías, J. Herrero-Martín, J. Stankiewicz. Phys. Rev. B **77**, *5*, 054107 (2008).
[2] Z. Wang, R. Gao, X. Deng, G. Chen, W. Cai, C. Fu. Ceram. Int. **45**, *2*, 1825 (2019).
[3] L. Wang, Z. Yang, J. Wu, M.E. Bowden, W. Yang, A. Qiao, Y. Du. npj Mater. Degrad. **4**, 16 (2020).
[4] L. Huang, L. Cheng, S. Pan, Y. He, C. Tian, J. Yu, H. Zhou. Ceram. Int. **46**, *17*, 27352 (2020).
[5] V. Sedykh, O. Rybchenko, V. Rusakov, S. Zaitsev, O. Barkalov, E. Postnova, T. Gubaidulina, D. Pchelina, V. Kulakov. J. Phys. Chem. Solids **171**, 111001 (2022).
[6] V. Sedykh, V. Rusakov, O. Rybchenko, A. Gapochka, K. Gavrilicheva, O. Barkalov, S. Zaitsev, V. Kulakov. Ceram. Int. **49**, *15*, 25640 (2023).
[7] V.D. Sedykh, O.G. Rybchenko, N.V. Barkovsky, A.I. Ivanov, V.I. Kulakov. FTT **63**, *10*, 1648 (2021) (in Russian).
[8] M. Takano, J. Kawachi, N. NAkanishi, Y. Taked. J. Solid State Chem. **39**, *1*, 75 (1981).
[9] A.I. Dmitriev, S.V. Zaitsev, M.S. Dmitrieva, O.G. Rybchenko, V.D. Sedykh. FTT **66**, *3*, 386 (2024). (in Russian).
[10] A.I. Dmitriev, S.V. Zaitsev, M.S. Dmitrieva. PZhTF **50**, *13*, 24, (2024) (in Russian).
[11] J.B. Yang, W.B. Yelon, W.J. James, Z. Chu, M. Kornecki, Y.X. Xie, X.D. Zhou, H.U. Anderson, A.G. Joshi, S.K. Malik. Phys. Rev. B **66**, *18*, 184415 (2002).
[12] G.B. Wright. Light Scattering Spectra of Solids. Springer Berlin, Heidelberg (1969). 763 p.
[13] O.I. Barkalov, S.V. Zaitsev, V.D. Sedykh. Solid State Comm. **354**, *1*, 114912 (2022).
[14] M.O. Ramirez, M. Krishnamurthi, S. Denev, A. Kumar, S.-Y. Yang, Y.-H. Chu, E. Saiz, J. Seidel, A.P. Pyatakov, A. Bush, D. Viehland, J. Orenstein, R. Ramesh, V. Gopalan. Appl. Phys. Lett. **92**, *2*, 022511 (2008).
[15] M.C. Weber, M. Guennou, H.J. Zhao, J. Iniguez, R. Vilarinho, A. Almeida, J.A. Moreira, J. Kreisel. Phys. Rev. B **94**, *21*, 214103 (2016).

Translated by A.Akhtyamov